

## Detection of the second harmonics of Lamb waves in fatigued magnesium plates

Makoto Fukuda<sup>1,\*</sup>, Kazuhiko Imano<sup>1</sup>, Hideki Yamagishi<sup>2</sup> and Katsuhiko Sasaki<sup>2</sup>

<sup>1</sup>Department of Electrical and Electronic Engineering, Graduate School of Engineering and Resource Science, Akita University, 1-1 Tegata Gakuen-machi, Akita, 010-8502 Japan

<sup>2</sup>Central Research Institute, Toyama Industrial Technology Center, 150 Futagami-cho, Takaoka, 933-0981 Japan

(Received 27 May 2011, Accepted for publication 26 July 2011)

**Keywords:** Second harmonic ultrasonic waves, Lamb wave, Fatigue test, Pure magnesium plate

**PACS number:** 43.25.Dc, 43.35.Zc [doi:10.1250/ast.32.271]

### 1. Introduction

Magnesium has recently been used as a weight-saving material in notebook personal computers or component parts of cars. This follows research on the mechanical behavior of magnesium as deformations and cracks result in significant accidents. Yamagishi *et al.* have reported on the mechanical properties of magnesium during cycle fatigue test using longitudinal ultrasonic waves and shear vertical (SV) waves [1,2]. The ultrasonic velocities and the Young and shear moduli had decreased significantly with increased loading in fatigue tests. Moreover, the existence of cracks in fatigued magnesium plate had been confirmed by scanning electron microscope (SEM).

Ultrasonic waves have been widely used in non-destructive evaluations (NDE) of various materials. Recently, measurements using plate waves, such as Lamb waves or Rayleigh waves, have been applied in the NDE field [3-5]. Most NDE methods that use longitudinal waves operate as point-to-point inspection methods. Plate wave measurements can, however, be taken over a wide distance in one time measurement. Thus more information can be obtained using plate wave methods compared with point-to-point inspection methods.

Infinitesimally small amplitude ultrasonic pulse waves, which are useful for finding open cracks, are used in most conventional NDE methods. However, dislocations and closed cracks are not easily detected. Recently, nonlinear ultrasonic (second harmonic or sub-harmonic) pulse waves have been studied for use in NDE [6-14]. The second harmonic frequency component  $2f_0$  ( $= 1$  MHz,  $f_0 = 500$  kHz in this paper) is generated in nonlinear vibrations of dislocations, closed cracks, and surfaces of solids, in a process called contact acoustic nonlinearity (CAN) for the finite-amplitude ultrasonic waves with fundamental  $f_0$ . Several studies of nonlinearity using Lamb waves have been conducted. Deng and coworkers [15-21], and Jacobs and coworkers [22,23] have measured nonlinear parameters of materials using Lamb wave. Kundu *et al.* have reported on detection of the "kissing bond," i.e., the bond at the interface between two surfaces in cracks [24]. Moreover, Morvan *et al.* have explained mode conversion of Lamb waves [25].

In this paper, Lamb waves are transmitted through pure magnesium plates subjected to various degrees of fatigue testing and the second harmonic components generated within the plates are detected. Increase in second harmonic components and its possible use in determining mechanical properties of magnesium are discussed.

### 2. Propagation of Lamb waves

#### 2.1. Generation of Lamb waves

The propagation mode of a Lamb wave in a plate depends on both the thickness  $d$  of the material and the frequency  $f$  of the ultrasonic waves. The propagation velocities of these waves can be calculated using the Rayleigh-Lamb equations [26]. Lamb waves can be divided into two kinds of mode; the symmetrical mode (S mode) and asymmetrical mode (A mode). The difference between the two is that the vibration of displacement and velocity over the plate surfaces are symmetric in the S mode and asymmetric in the A mode. Each mode continues to propagate in that mode if the plate maintains the same thickness and uniform properties. Therefore, if other modes such as second harmonic components are generated, the presence of non-uniform features such as dislocations and closed cracks can be determined.

Dispersion curves of the phase velocity  $c_p$  and group velocity  $c_g$  in a magnesium plate (longitudinal wave velocity  $c_L = 5,930$  m/s, shear wave velocity  $c_T = 3,070$  m/s, and thickness  $d = 5.5$  mm) are shown in Figs. 1(a) and (b), respectively. Lamb waves can be effectively excited when the incident angle  $\theta_c$  satisfies the phase matching condition [3]. This angle is calculated from Snell's law as

$$\theta_c = \sin^{-1} \frac{c_w}{c_p} \quad (1)$$

where  $c_w$  ( $= 2,430$  m/s) is the ultrasonic wave velocity in the wedge. Dispersion curves for the critical angle in the magnesium plate are easily calculated. A frequency of  $f = 500$  kHz is selected in the generation of the S0 mode Lamb waves, based on the following reasons; (1) the S0 mode Lamb waves can be easily generated compared with high-order Lamb waves, and (2) since the group velocity of S0 mode Lamb waves is relatively slow ( $c_g = 2,000$  m/s), magnesium plates can be used as propagation distances of Lamb waves is relatively short. The incident angle  $\theta_c$  can

\*e-mail: mfukuda@gipc.akita-u.ac.jp

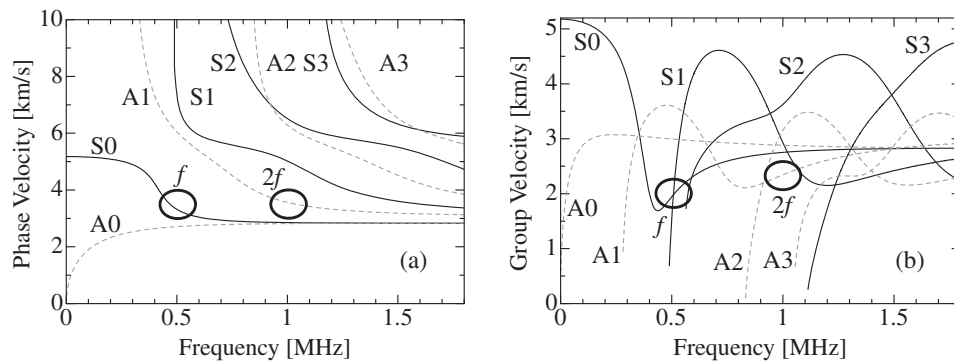


**Fig. 1** Dispersion curves of (a) the phase velocity  $c_p$  and (b) the group velocity  $c_g$  for Lamb waves in the magnesium plate. Solid lines are S mode Lamb waves and dashed lines are A mode Lamb waves, respectively.

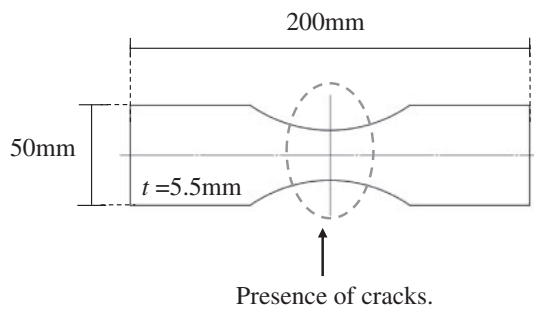


**Fig. 2** Form of magnesium plates.

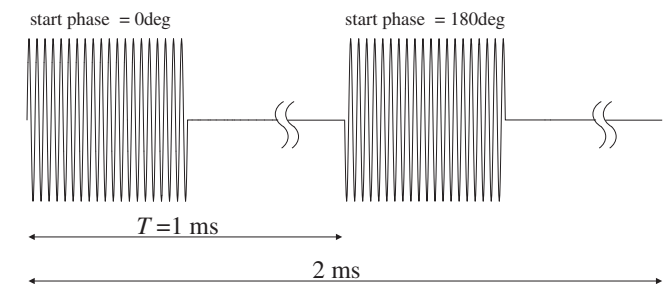


**Fig. 3** Applied signal to the transducer.

be evaluated using  $c_p$  (3,200 m/s) and  $c_w$  (2,430 m/s) at approximately 50 degrees.

### 2.2. Structure of transducer

For the effective generation of S0 mode Lamb waves in the magnesium plate, a 50-degree wedge was then inserted between the piezoelectric transducer and the magnesium plate. The wedge was made of epoxy resin ( $c_w = 2,430$  m/s). Both transmitting and receiving transducers were thickness-mode piezoelectric transducer ( $\text{PbTiO}_3$ ) disks with resonance frequencies of 500 kHz and 1 MHz, respectively. The transducers and wedges were fabricated with silver paint to act as electrical leads.

## 3. Experimental

### 3.1. Magnesium plates

The material under study was pure magnesium. The magnesium plates, diagrammed in Fig. 2, were extruded perpendicular to the longitudinal direction. The samples were subjected to cyclic tensile-stress under controlled conditions. The stress-amplitude,  $\sigma_a$ , was 28.3 MPa, the stress ratio,  $R$ , was 0, and the frequency was 30 Hz, which were controlled by a hydraulic servo fatigue tester (FT-5; Saginomiya, Tokyo, Japan) at room temperature. The fatigued samples were prepared separately using a varied number of cycles, where sample No. 1 had 0 cycles, sample No. 2 had  $1 \times 10^5$  cycles, and sample No. 3 had  $2 \times 10^5$  cycles.

In the previous report, the material has been suggested to develop many closed cracks at the grain boundary, which influence the ultrasonic waves strongly. The material used in

this study was from the same lot number as the previous studies, i.e., the NDE system in this study should be also affected by the defects as well as the ordinary lattice defects such as dislocations and twinning.

### 3.2. Pulse inversion averaging

In our system, the pulse inversion averaging (PIA) method [27] was applied to enhance the second harmonic component. Two pulse waves of opposite phase were transmitted alternately in the PIA method illustrated in Fig. 3. The waves were time-averaged to cancel out the fundamental and odd harmonic components of the waves. The driving voltage waveform (as shown in Fig. 3) for the PIA was produced in an arbitrary waveform generator (Hewlett Packard, HP33120A) and designed for 20 cycles of a 500 kHz burst sine wave (burst duration time: 40  $\mu\text{s}$ ). After an appropriate interval,  $T$ , the next inverted signal was applied to the transducer. That interval was determined to be 1 ms; PIA was automatically carried out by averaging every interval  $T$ .

### 3.3. Experimental setup

The experimental set-up is shown schematically in Fig. 4. Transmission signals were generated using an arbitrary waveform generator and their amplitudes were amplified to 100 V with a bipolar power amplifier (NF Corporation, BA4825). These signals were applied to the 500 kHz transducer. Ultrasonic pulses of 500 kHz were transmitted through the magnesium plate via the epoxy resin wedge. S0 mode Lamb waves were generated as ultrasonic pulse waves propagated through the magnesium plates. The second harmonic components of the Lamb waves were generated by the nonlinear vibrations of the closed cracks and were

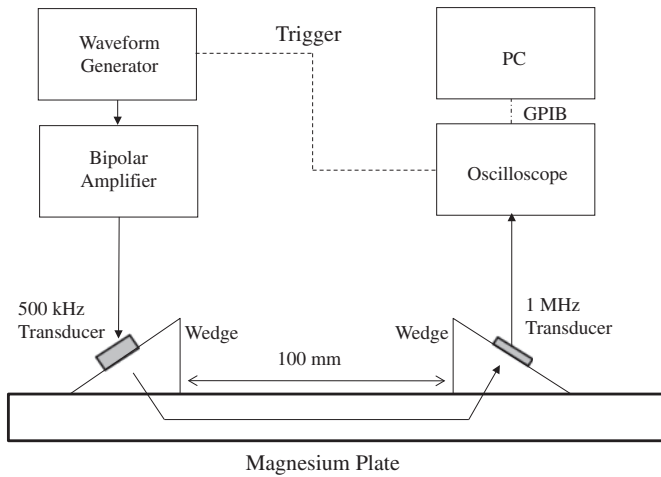


**Fig. 4** Experimental setup.

received by the 1 MHz transducer. The resultant pulse waveform and spectrum were captured by an oscilloscope (Agilent, Infiniium 54845A) and the second harmonic components could be observed in real time using the FFT function of the oscilloscope. Finally, the received pulse waveforms were digitized and fed into a personal computer via a general purpose interface bus (GPIB).

In this study, each transducer was set 50 mm away from the center of the magnesium plate; i.e. the propagation distance for the Lamb waves was 100 mm.

**4. Results and discussion**

Typical received waveforms and spectra before PIA are shown in Fig. 5. Second harmonic components were confirmed, although these were of smaller intensity than the fundamental components. Figure 6 shows received waveforms and spectra after PIA. The fundamental components

have been removed compared with those waveforms before PIA was performed. Figures 6(a) and (b) show results from plate No. 1. The second harmonic component in Fig. 6(b) would be cumulatively generated as the Lamb waves were propagated. This was the more commonly generated component in all three plates. Figures 6(c) and (d) show respectively the results of a received waveform in No. 2 plate and its spectrum. The second harmonic component is seen in Fig. 6(d) to have been increased by 3 dB compared with that in plate No. 1 [Fig. 6(b)]. The signal would be generated from dislocations and closed cracks caused by the fatigue tests. Figures 6(e) and (f) shows similar results for plate No. 3. Here the second harmonic component in Fig. 6(f) has increased by 6 dB compared to plate No. 1 [Fig. 6(b)]. Second harmonic components have thus increased as the fatigue test cycles were increased.

To determine the Lamb wave mode of the received waveform a wavelet transformation was performed and the result was compared with dispersion curves of group velocity. Using the waveforms in Figs. 6(a) and 6(e), these transformation results for plates No. 1 and No. 3 are shown in Figs. 7(a) and 7(b). The shaded area corresponded to the existence of frequency components on the time axis. In the plate No. 1 (Fig. 7(a)), without fatigue test, second harmonic component of S0 mode Lamb waves were mainly detected, since the second harmonic component was cumulatively generated as the Lamb waves were propagated because the fatigue test was not carried out. The group velocity of the generated second harmonic waves differed from the fundamental one and the mass of second harmonic waves, shaded area, was slightly shifted to the dispersion curve of A1 mode Lamb wave. Lamb wave of the double frequency having the same phase velocity as that of the fundamental Lamb wave is generated as the second harmonic Lamb wave [22,23]. Namely, A1 mode Lamb waves (1 MHz) having the same phase velocity (approximately 3200 m/s) as that of S0 mode

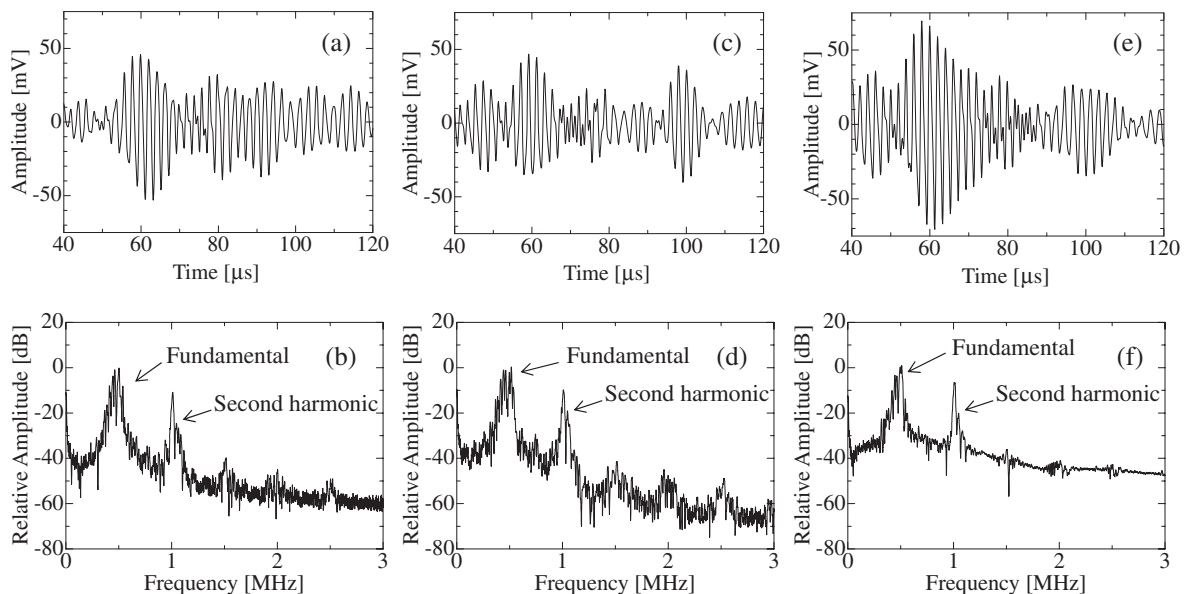


**Fig. 5** Results before PIA: (a) received waveform in No. 1 and (b) its spectrum; (c) received waveform in No. 2 and (d) its spectrum; (e) received waveform in No. 3 and (f) its spectrum.

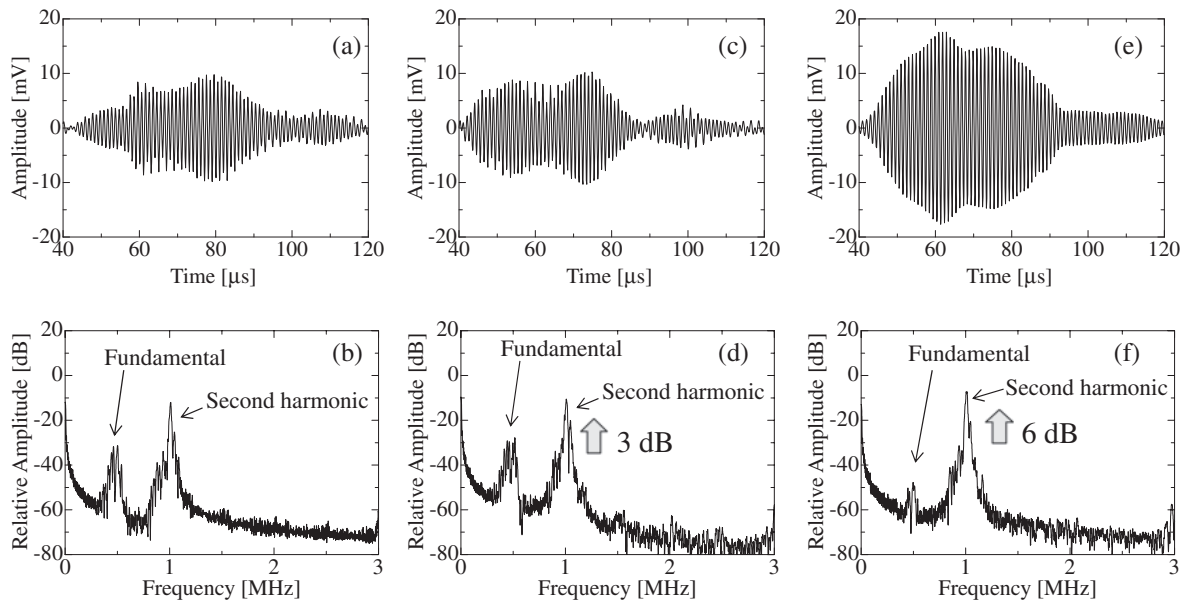


Fig. 6 Waveform results after PIA. The order follows that for Fig. 5.

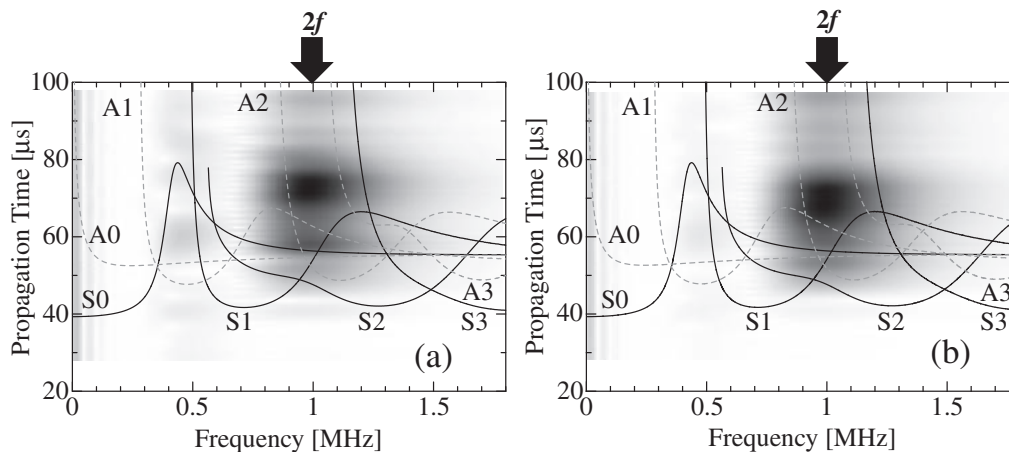


Fig. 7 Results of wavelet transformations for received waveforms from plates No. 1 and No. 3 after PIA.

Lamb waves (500 kHz) as shown in Fig. 1(a) were generated. On the other hand, in the plate No. 3 (Fig. 7(b)), dislocations and closed cracks were created. When the fundamental Lamb waves (S0 mode) propagate to the plate, the second harmonic Lamb waves (A1 mode) are generated by nonlinear vibration of the cracks. Second harmonic components were generated at earlier time (approximately 65  $\mu\text{s}$ ) compared with the plate No. 1 (approximately 70  $\mu\text{s}$ ), which nonlinear vibration source was located nearby the transducer for transmitting ultrasonic wave compared with cumulative propagating nonlinearity. As the results, it confirmed that the second harmonic components generated from the magnesium plates were increased by the fatigue test.

## 5. Conclusions

Lamb waves of finite amplitude were generated in pure magnesium plates with varying distribution of dislocations and closed cracks. Second harmonic components had increas-

ed as the number of fatigue test cycles producing the stress faults was increased. At 200 thousand cycles, second harmonic components had increased by approximately 6 dB compared with an unstressed plate. From these results, we confirmed that second harmonic components had been effectively detected dislocations and closed cracks in the magnesium plates.

For the future, structural analysis of sections through these plates will be performed to identify the source of the second harmonic pulse waves.

## Acknowledgement

This work was partially supported by Ono Acoustics Research Fund in 2010.

## References

- [1] H. Yamagishi, M. Fukuhara and A. Chiba, "Determination of the cyclic-tension fatigue of pure magnesium using multiple

- ultrasonic waves,” *Mater. Trans.*, **51**, 1255–1263 (2010).
- [2] H. Yamagishi, M. Fukuhara and A. Chiba, “Determination of the mechanical properties of extruded pure magnesium during tension-tension low-cycle fatigue using ultrasonic testing,” *Mater. Trans.*, **51**, 2025–2032 (2010).
- [3] K. Imano, “Experimental study on the mode conversion of Lamb waves in a metal plate of stepped thickness using optical detection,” *Soc. Mater. Eng. Resour. Jpn.*, **17**, 201–204 (2010).
- [4] K. Imano and M. Kondou, “Possibilities of nondestructive evaluation of a pipe using air-coupled ultrasonic wave in the MHz range,” *IEICE Electron. Exp.*, **5**, 668–671 (2008).
- [5] K. Imano, “A tilted angle polarization type piezoelectric transducer for plate wave generation,” *IEICE Electron. Exp.*, **4**, 340–343 (2007).
- [6] M. Fukuda, M. Nishihira and K. Imano, “Novel detection system using double-layered piezoelectric transducer in same polarization direction for sub-harmonic components generated from plastic-deformed metal rod,” *Jpn. J. Appl. Phys.*, **47**, 3899–3903 (2008).
- [7] M. Fukuda, M. Nishihira and K. Imano, “Real time detection of second-harmonic components generated from plastic-deformed metal rod using double-layered piezoelectric transducer,” *Jpn. J. Appl. Phys.*, **46**, 4529–4531 (2007).
- [8] K. Imano and A. Muto, “Detection of second harmonic wave from the closed crack using finite amplitude ultrasonic wave,” *J. Soc. Mater. Eng. Resour. Jpn.*, **20**, 12–18 (2007) (in Japanese).
- [9] Y. Ohara, S. Yamamoto, T. Mihara and K. Yamanaka, “Ultrasonic evaluation of closed cracks using subharmonic phased array,” *Jpn. J. Appl. Phys.*, **47**, 3908–3915 (2008).
- [10] K. Kawashima, M. Murase, K. Shibata and T. Ito, “Back-scattered transverse wave imaging of cracked-faces with linear and nonlinear ultrasonics,” *Mater. Trans.*, **48**, 1202–1207 (2007).
- [11] T. Ohatani, K. Kawashima, M. Drew and P. Guagliard, “Nonlinear acoustic evaluation of creep damage in boiler heat exchange tubes,” *Jpn. J. Appl. Phys.*, **46**, 4577–4582 (2007).
- [12] J. H. Cantrell, “Dependence of microelastic-plastic nonlinearity of martensitic stainless steel on fatigue damage accumulation,” *J. Appl. Phys.*, **100**, 063508-1-7 (2006).
- [13] A. Alippi, A. Bettucci, M. Germano and D. Passeri, “Harmonic and subharmonic acoustic wave generation in finite structures,” *Ultrasonics*, **44**, e1313–e1318 (2006).
- [14] I. Solodov and C. A. Vu, ““Popping” nonlinearity and chaos in vibrations of a contact interface between solids,” *Acoust. Phys.*, **39**, 476–479 (1993).
- [15] M. Deng and J. Pei, “Assessment of accumulated fatigue damage in solid plates using nonlinear Lamb wave approach,” *Appl. Phys. Lett.*, **90**, 121902-1-3 (2007).
- [16] M. Deng and J. Yang, “Characterization of elastic anisotropy of a solid plate using nonlinear Lamb wave approach,” *J. Sound Vib.*, **308**, 201–211 (2007).
- [17] M. Deng, P. Wang and X. Lv, “Influences of interfacial properties on second-harmonic generation of Lamb waves propagating in layered planar structures,” *J. Phys. D: Appl. Phys.*, **39**, 3018–3025 (2006).
- [18] M. Deng, “Characterization of surface properties of a solid plate using nonlinear Lamb wave approach,” *Ultrasonics*, **44**, e1157–e1162 (2006).
- [19] M. Deng, “Analysis of second-harmonic generation of Lamb waves propagating in layered planar structures with imperfect interfaces,” *Appl. Phys. Lett.*, **88**, 221902-1-3 (2006).
- [20] M. Deng, P. Wang and X. Lv, “Experimental verification of cumulative growth effect of second harmonic of Lamb wave propagation in an elastic plate,” *Appl. Phys. Lett.*, **86**, 124104-1-3 (2005).
- [21] M. Deng, P. Wang and X. Lv, “Experimental observation of cumulative second-harmonic generation of Lamb-wave propagation in an elastic plate,” *J. Phys. D: Appl. Phys.*, **38**, 344–353 (2005).
- [22] C. Pruell, J. Kim, J. Qu and L. J. Jacobs, “Evaluation of plasticity driven material damage using Lamb waves,” *Appl. Phys. Lett.*, **91**, 231911-1-3 (2007).
- [23] C. Bemes, J. Kim, J. Qu and L. J. Jacobs, “Dynamic range of nanoresonators with random rough surfaces in the presence of thermomechanical and momentum exchange noise,” *Appl. Phys. Lett.*, **90**, 021901-1-3 (2007).
- [24] T. Kundu, A. Maji, T. Ghosh and K. Maslov, “Detection of kissing bonds by Lamb waves,” *Ultrasonics*, **35**, 573–580 (1998).
- [25] B. Morvan, A. Hladky-Hennion, D. Leduc and J. Izbicki, “Ultrasonic guided waves on a periodical grating: Coupled modes in the first Brillouin zone,” *J. Appl. Phys.*, **101**, 114906-1-7 (2007).
- [26] H. Nishino, “Fundamental and application of ultrasonic guided wave for nondestructive inspection,” *Hihakai Kensa*, **52**, 654–661 (2003) (in Japanese).
- [27] M. Fukuda, M. Nishihira and K. Imano, “Real time extraction system using double-layered piezoelectric transducer for second-harmonic ultrasonic pulse waves,” *Jpn. J. Appl. Phys.*, **45**, 4556–4559 (2006).